Transcription factor ATF5 is required for terminal differentiation and survival of olfactory sensory neurons

Shu-Zong Wang[a,b], Jianhong Ou[b], Lihua J. Zhu[b,c], and Michael R. Green[a,b,1]

[a]Howard Hughes Medical Institute, [b]Programs in Gene Function and Expression and Molecular Medicine, and [c]Program in Bioinformatics and Integrative Biology, University of Massachusetts Medical School, Worcester, MA 01605

Edited by Solomon H. Snyder, The Johns Hopkins University School of Medicine, Baltimore, MD, and approved September 27, 2012 (received for review June 21, 2012)

Activating transcription factor 5 (ATF5) is a member of the ATF/cAMP response element-binding family of transcription factors, which compose a large group of basic region leucine zipper proteins whose members mediate diverse transcriptional regulatory functions. ATF5 has a well-established prosurvival activity and has been found to be overexpressed in several human cancers, in particular glioblastoma. However, the role(s) of ATF5 in development and normal physiology are unknown. Here we address this issue by deriving and characterizing homozygous *Atf5* knockout mice. We find that *Atf5*$^{-/-}$ pups die neonatally, which, as explained below, is consistent with an olfactory defect resulting in a competitive suckling deficit. We show that *Atf5* is highly expressed in olfactory sensory neurons (OSNs) in the main olfactory epithelium starting from embryonic stage 11.5 through adulthood. Immunostaining experiments with OSN-specific markers reveal that ATF5 is expressed in some immature OSNs and in all mature OSNs. Expression profiling and immunostaining experiments indicate that loss of *Atf5* leads to a massive reduction in mature OSNs resulting from a differentiation defect and the induction of apoptosis. Ectopic expression of *Atf5* in neural progenitor cells induces expression of multiple OSN-specific genes. Collectively, our results suggest a model in which *Atf5* is first expressed in immature OSNs and the resultant ATF5 functions to promote differentiation into mature OSNs. Thus, ATF5 is required for terminal differentiation and survival of OSNs.

hyposmia | olfaction | neonatal death | olfactory marker protein | TUJ1

Activating transcription factor 5 (ATF5; also known as ATFx) is a member of the ATF/cAMP response element-binding (CREB) family of transcription factors, which compose a large group of basic region leucine zipper (bZIP) proteins whose members mediate diverse transcriptional regulatory functions (reviewed in ref. 1). A role for ATF5 in promoting cell survival was first suggested from expression profiling experiments, which revealed that *Atf5* was the gene most down-regulated in interleukin-3–dependent murine hematopoietic cells following apoptosis induction elicited by cytokine deprivation (2). Functional experiments demonstrated that the prosurvival function of ATF5 results from its ability to inhibit apoptosis (3).

A variety of subsequent studies have shown that ATF5 is overexpressed in, and contributes to the survival of, several human cancer cell lines and solid tumors, in particular glioblastoma (4, 5). The high level of ATF5 in brain tumors, coupled with the absence of *ATF5* expression in mature neurons, has raised the possibility that ATF5 may be a therapeutic target for treatment of glioblastoma. Consistent with this idea, inhibiting ATF5 function, using either a dominant-negative mutant or a small interfering RNA, causes massive apoptotic death of rodent and human glioblastoma cell lines. By contrast, comparable loss of ATF5 function does not affect survival of cultured neurons or glial cells (6, 7).

A rigorous evaluation of the role of ATF5 as a therapeutic target requires a clear understanding of normal ATF5 function. However, the role of ATF5 in development and physiology has not been determined. Here we address this issue by deriving and characterizing *Atf5*$^{-/-}$ mice.

Results

Derivation of *Atf5*$^{-/-}$ Mice. To investigate the physiological role of ATF5, we derived *Atf5*$^{-/-}$ mice. The gene-targeting strategy involved replacing almost the entire coding region of *Atf5* with a LacZ-Neo cassette, such that the *LacZ* gene is under the control of the endogenous *Atf5* promoter (Fig. S1*A*). The genomic structure of the *Atf5* locus in *Atf5*$^{+/+}$, *Atf5*$^{+/-}$, and *Atf5*$^{-/-}$ mice was confirmed by Southern blot (Fig. S1*A*) and PCR (Fig. S1*B*) analyses. As expected, *Atf5* expression was lost in mouse embryonic fibroblasts derived from *Atf5*$^{-/-}$ mice and in the liver (Fig. S1*C*) and olfactory epithelium (OE) of *Atf5*$^{-/-}$ mice (Figs. S1*D* and S2*C*).

***Atf5*$^{-/-}$ Mice Undergo Neonatal Death.** At birth (postnatal day 0, P0), no major phenotypic differences were observed between *Atf5*$^{+/+}$, *Atf5*$^{+/-}$, and *Atf5*$^{-/-}$ pups, and the ratio of all three genotypes was consistent with the predicted Mendelian distribution (Fig. 1*A*). Likewise, as expected, the genotypes of embryonic stage day 14 (E14) embryos were consistent with the predicted Mendelian distribution.

Significantly, however, following birth mice lacking *Atf5* failed to thrive, as evidenced by the drastic reduction in the percentage of *Atf5*$^{-/-}$ pups between P0 and P6 (Fig. 1*A*). The results of Fig. 1*B* show that within 48 h after birth the majority (11/14) of *Atf5*$^{-/-}$ pups died, whereas no neonatal death was observed in *Atf5*$^{+/+}$ mice. Further analysis of the dead *Atf5*$^{-/-}$ mice revealed a lack of milk in their stomach (Fig. 1*C*), consistent with the possibility of a competitive suckling deficit. Despite similar weights at birth, the weight of the few surviving *Atf5*$^{-/-}$ pups was less than that of their wild-type siblings throughout 10 wk after birth (Fig. 1*D*).

High Selective Expression of *Atf5* in the Olfactory System. As a first step toward determining why loss of *Atf5* results in neonatal lethality, we performed a series of experiments to analyze *Atf5* expression. In *Atf5*$^{+/-}$ and *Atf5*$^{-/-}$ mice, *LacZ* transcription is directed by the *Atf5* promoter (Figs. S1*A* and S2*A*), and thus β-galactosidase (β-gal) activity provides a convenient readout of *Atf5* expression. The whole-mount β-gal activity assay of Fig. 2*A* shows that in an *Atf5*$^{+/-}$ mouse at E14.5, *Atf5* was highly and specifically expressed in the nasal cavity. To confirm that the β-gal expression pattern faithfully recapitulated that of endogenous *Atf5*, we performed in situ hybridization. The results in Fig. S2*B* show

Author contributions: S.-Z.W. and M.R.G. designed research; S.-Z.W. performed research; S.-Z.W., J.O., L.J.Z., and M.R.G. analyzed data; and S.-Z.W. and M.R.G. wrote the paper.

The authors declare no conflict of interest.

This article is a PNAS Direct Submission.

Data deposition: The data reported in this paper have been deposited in the Gene Expression Omnibus (GEO) database, www.ncbi.nlm.nih.gov/geo (accession no. GSE37609).

[1]To whom correspondence should be addressed. E-mail: michael.green@umassmed.edu.

This article contains supporting information online at www.pnas.org/lookup/suppl/doi:10.1073/pnas.1210479109/-/DCSupplemental.

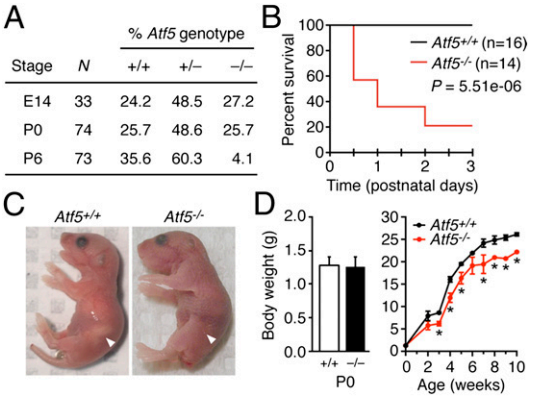

Fig. 1. *Atf5*$^{-/-}$ mice undergo neonatal death. (*A*) Percentage of viable *Atf5* genotypes among E14 embryos and newborn (P0) and 6-d-old (P6) pups. *n*, number of pups examined. (*B*) Kaplan–Meier survival curve of *Atf5*$^{+/+}$ and *Atf5*$^{-/-}$ mice up to 3 d after birth. (*C*) Images showing *Atf5*$^{+/+}$ and *Atf5*$^{-/-}$ mice 24 h after birth. In *Atf5*$^{+/+}$ mice, the arrow points to the milk spot, which is absent in *Atf5*$^{-/-}$ mice. (*D*) Body-weight analysis of *Atf5*$^{+/+}$ and surviving *Atf5*$^{-/-}$ pups at P0 (*Left*) and over the first 10 wk (*Right*). *$P < 0.05$.

that, like β-gal, *Atf5* was highly and specifically expressed in the nasal cavity.

The nasal cavity is composed of two types of epithelia, respiratory and olfactory epithelia (reviewed in ref. 8). To determine which epithelial type is the site of *Atf5* expression, we performed a whole-mount β-gal activity assay on sagittal head sections of an *Atf5*$^{+/-}$ P30 mouse. Fig. 2*A* (*Right*) shows that β-gal activity was restricted to the olfactory system, including the both the turbinates and the septum of the main OE (hereafter referred to as the OE), the vomeronasal organ (VNO), the Grueneberg ganglion, the septal organ, and the olfactory bulb (OB). In situ hybridization confirmed that *Atf5* was expressed in the OE (Fig. S2*C*) and VNO (Fig. S2*D*). Expression of *Atf5* in the OE and OB was also detected by immunostaining for β-gal (Fig. 2*B* and see Fig. S3 below).

We next analyzed *Atf5* expression at a series of different developmental stages. We found that *Atf5* was selectively expressed in the olfactory system from as early as E11.5 (Fig. 2*C*). Expression of *Atf5* in the olfactory system remained strong through adulthood (up to 10 mo tested so far; Fig. S2*E*). In addition, we found that *Atf5* expression was restricted to the olfactory system through adulthood. Taken together, these results demonstrate that *Atf5* is highly expressed in the olfactory system from early development (E11.5) through adulthood, suggesting an important role in olfactory function.

***Atf5* Is Selectively Expressed in Olfactory Sensory Neurons.** To identify the cell type that expresses *Atf5*, a β-gal activity assay was performed on horizontal sections of the nasal cavity. Fig. 3*A* shows that *Atf5* expression was localized between the sustentacular and the basal cell layers, an area that corresponds to the region where olfactory sensory neurons (OSNs), both immature and mature, reside.

To delineate the specific cell type(s) that expresses *Atf5*, we performed double immunostaining for β-gal and specific OE markers. TUJ1 (also called TUBB3) is a well-established marker that is strongly expressed in immature OSNs and weakly expressed in mature OSNs (9). Fig. 3*B* (*Upper*) shows that, in the OE, many TUJ1+ cells, particularly those located near the basal layer, did not costain with β-gal (Fig. S3 *A* and *B*). Significantly, however, some β-gal+ cells also stained strongly for TUJ1. The staining pattern of GAP43, an alternative marker of immature OSNs (10), was very similar to that observed for TUJ1 (Fig. S4).

We also performed coimmunostaining for OMP, a characteristic marker of mature OSNs (9). We found that in the OE, all OMP+ neurons, which reside near the apical surface of the OE, were also β-gal+ (Fig. 3*B*, *Lower*, and Fig. S3 *A* and *C*). Similar results were obtained in adult mice (Fig. S3*D*). Taken together, the results described above demonstrate that *Atf5* is expressed in some immature (TUJ1+) and in all mature (OMP+) OSNs.

We performed comparable double immunostaining experiments for the VNO and OB. For the VNO, we found that *Atf5* expression, as evidenced by β-gal staining, was also found in both TUJ1+ and OMP+ vomeronasal sensory neurons (VSNs) (Fig. 3*C*). For the OB, strong β-gal+ staining was confined to the outer, glomerular layer, which contains axons from OSNs that reside in the OE (Fig. 3*D* and Fig. S3*E*).

ATF5 Is Required for Terminal Differentiation of OSNs. The highly restricted expression pattern of *Atf5* in the olfactory system strongly suggested that *Atf5* has an important role in OSNs. To test this possibility, we first compared gene expression profiles of OE from *Atf5*$^{+/+}$ and *Atf5*$^{-/-}$ mice. Briefly, olfactory turbinates and septum, where the main OE is located, were dissected and collected from three different litters of *Atf5*$^{+/+}$ and *Atf5*$^{-/-}$ P0 pups, and total RNA was isolated from each sample and subjected to microarray analysis. Using ≥1.5-fold as a threshold and $P < 0.001$ as a cutoff, the microarray results revealed that the expression levels of 274 genes were significantly decreased in *Atf5*$^{-/-}$ OE (Fig. S5 and Dataset S1). Fig. 4*A* presents a heat map of the 40 genes whose expression levels were decreased most substantially in *Atf5*$^{-/-}$ OE. Notably, among the 274 genes with decreased expression levels, ~85% were associated with neuronal function including essential components of the canonical olfactory signal transduction pathway, such as multiple olfactory receptor (*Olfr*) genes, the olfactory-specific G protein *Gnal* (also known as *Golf*), the guanine nucleotide-binding protein *Gng13*, the adenylate cyclase *Adcy3*, the cyclic nucleotide gated channel *Cnga2*, and the calcium-activated chloride channel *Ano2* (11).

To validate the microarray results, we selected 20 genes that were among the most affected by loss of *Atf5* and analyzed their

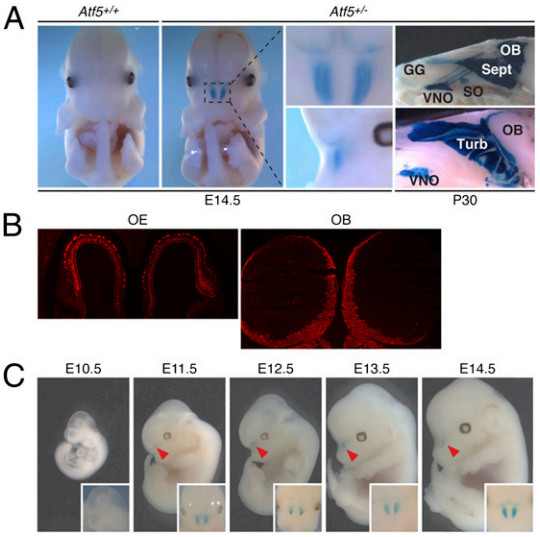

Fig. 2. High, selective expression of *Atf5* in the olfactory system. (*A*) Whole-mount β-gal activity assay. (*Left*) Front views of β-gal activity in *Atf5*$^{+/+}$ and *Atf5*$^{+/-}$ E14.5 embryos. Close-up views of β-gal activity in the *Atf5*$^{+/-}$ embryo (dashed box) are shown from front and side. (*Far Right*) Whole-mount β-gal activity assay on two different sagittal head sections of a P30 *Atf5*$^{+/-}$ mouse. GG, Grueneberg ganglion; OB, olfactory bulb; Sept, septum; SO, septal organ; Turb, turbinates; VNO, vomeronasal organ. Magnification 5×. In the *Upper* but not *Lower* image at *Far Right*, the surface of the OB has been maintained, accounting for the apparent differences in β-gal staining. Enlarged images are shown in Fig. S8*A*. (*B*) Immunofluorescence monitoring β-gal staining in the OE and OB of a P0 *Atf5*$^{+/-}$ pup. Magnification 50×. (*C*) Whole-mount β-gal activity assay on *Atf5*$^{+/-}$ E10.5–E14.5 embryos (arrowheads point to β-gal staining) (*Insets*, front view).

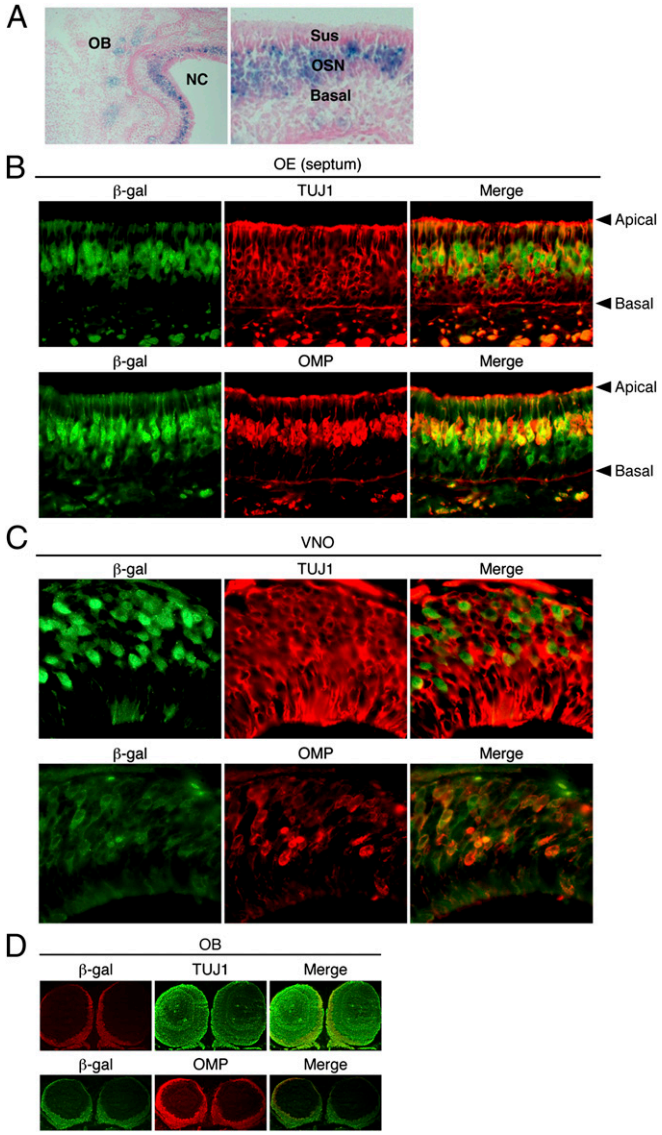

Fig. 3. *Atf5* is selectively expressed in OSNs. (*A*) β-Gal activity assay on a horizontal section of the nasal cavity of a P0 $Atf5^{-/-}$ pup, followed by eosin staining. Magnification 100× (*Left*) and 200× (*Right*). OB, olfactory bulb; NC, nasal cavity; Sus, sustentacular cells; OSN, olfactory sensory neurons; Basal, globose basal and horizontal basal cells. (*B–D*) Immunofluorescence monitoring β-gal, TUJ1, and OMP staining in coronal sections of the septum (*B*), VNO (*C*), and OB (*D*) of a P0 $Atf5^{+/-}$ pup. Merged images are shown on the *Right*. Arrowheads indicate the apical and basal layers of the OE. Magnification 200× (*B*), 400× (*C*), and 50× (*D*). Enlarged images of *D* are shown in Fig. S8*B*.

expression by quantitative RT-PCR (qRT-PCR). The results of Fig. 4*B* show that the expression levels of 19 of the 20 genes were significantly decreased in $Atf5^{-/-}$ OE. Several of these validated genes, including *Cnga2*, *Gnal*, *Gng13*, and *Rtp1*, are known to be essential for olfactory function (11). Notably, previous studies have shown that mice lacking *Gnal* (12), *Cnga2* (13), or *Adcy3* (14) are profoundly hyposmic and have a neonatal death phenotype comparable to that of $Atf5^{-/-}$ mice. qRT-PCR analysis of a representative set of OSN-specific genes indicated that their expression levels in $Atf5^{+/-}$ and $Atf5^{+/+}$ OE were comparable (Fig. S6*A*).

For comparison, we also analyzed expression of the neuronal progenitor markers *Ascl1* (also called *Mash1*) and *Neurog1* (also called *Ngn1*) and the immature OSN markers *Gap43*, *Stmn2* (also called *Scg10*), and *Tuj1* (Fig. 4*B*). Expression levels of *Ascl1* and *Neurog1* were not substantially reduced in $Atf5^{-/-}$ OE, indicating that OSN progenitors are not affected by loss of *Atf5*. Expression levels of *Gap43*, *Stmn2*, and *Tuj1* were modestly reduced, suggesting that some immature OSNs are affected by loss of ATF5, consistent with the immunostaining results demonstrating expression of *Atf5* in some but not all immature OSNs (Fig. 3*B*).

To confirm the expression profiling and qRT-PCR results, we performed immunostaining experiments. As expected, OMP staining was readily detectable in OE from $Atf5^{+/+}$ (Fig. 4*C*) as well as from $Atf5^{+/-}$ (Fig. S6*B*) mice. Fig. 4*C* shows that, in $Atf5^{-/-}$ OE, OMP staining was almost completely abolished, indicating a dramatic loss of mature OSNs (Fig. S6*B*). By contrast, the TUJ1 staining pattern of $Atf5^{+/+}$ and $Atf5^{-/-}$ OE was roughly comparable (Fig. 4*C*). Likewise, the GAP43 staining pattern of $Atf5^{+/-}$ and $Atf5^{-/-}$ OE was similar (Fig. S4).

ATF5 Is Critical for Survival of Mature OSNs. As described above, ATF5 is an anti-apoptotic factor, raising the possibility that ATF5 functions, at least in part, by preventing apoptosis and thereby promoting survival of OSNs. To investigate this possibility, we analyzed apoptosis in OE from $Atf5^{+/+}$ and $Atf5^{-/-}$ mice by immunostaining with an antibody to cleaved caspase 3. The results show that, in $Atf5^{+/+}$ (Fig. 5*A*) and $Atf5^{+/-}$ (Fig. S6*C*), OE apoptosis was virtually undetectable, consistent with previous reports (15, 16), whereas $Atf5^{-/-}$ OE contained a large number of apoptotic cells (Fig. 5*A* and Fig. S6*C*). Double immunostaining with TUJ1 revealed that apoptosis occurred in some immature OSNs, but most apoptotic cells did not stain strongly for TUJ1 and were in the apical region of OE that is normally occupied by mature OSNs (Fig. 5*A*). In contrast to the apoptosis results, there was no difference in cellular proliferation between $Atf5^{+/+}$ and $Atf5^{-/-}$ OE as evidenced by equivalent phospho-histone H3 staining (Fig. 5*B*).

ATF5 Can Direct OSN-Specific Gene Expression. Because ATF5 is a transcription factor, it seemed likely that ATF5 functions by stimulating expression of genes required for OSN maturation and survival. To test this idea, we asked whether ectopic expression of *Atf5* in rat Odora cells, which are derived from OSN progenitor cells and are an experimental model of OSN progenitors (17), would result in the transcriptional activation of OSN-specific genes. We tested a panel of 20 genes previously found to have decreased expression levels in $Atf5^{-/-}$ OE (Fig. 4 *A* and *B*). Myc- or Flag-tagged ATF5 were transiently expressed in Odora cells (Fig. S7*A*) and after 6 d qRT-PCR analysis revealed the up-regulation of a number of OSN-specific genes including *Ano2*, *Kirrel2*, *Olfr15*, *Olfr170*, *Olfr513*, and *Rtp1* (Fig. 6*A*).

We next performed similar experiments in murine neural stem cells, which were isolated from the lateral and medial ganglionic eminence of E14 mouse embryos. These cells are not the normal progenitor of OSNs and therefore provide a rigorous test for the ability of ATF5 to direct OSN-specific gene expression. After confirming stemness, as evidenced by expression of SOX2 and VIM (Fig. 6*B*, *Left*), and multipotency, as evidenced by the capacity to differentiate into GFAP+ astrocytes and TUJ1+ neurons (Fig. 6*B*, *Right*), we transduced neural stem cells with a retrovirus that expresses *Atf5* (Fig. S7*B*). After growth in differentiation medium for 6 d, qRT-PCR was performed to measure expression of the same panel of 20 genes that were analyzed in Fig. 6*A*. The results show that ectopic expression of *Atf5* resulted in up-regulation of a number of OSN-specific genes including *Kirrel2*, *Olfr15*, *Olfr170*, *Olfr513*, *Omp*, and *Rtp1* (Fig. 6*C*).

To ask whether some or all of the up-regulated genes were direct targets of ATF5, we performed chromatin-immunoprecipitation (ChIP) experiments. We analyzed four genes—*Kirrel2*, *Olfr170*, *Olfr513*, and *Rtp1*—that were induced by ectopic expression of ATF5 in both rat Odora and murine neural stem cells. ATF5 occupancy was analyzed by ChIP assays in Odora cells using a series of promoter-specific primers. The ChIP results of Fig. 6*D* show that ATF5 could be detected on both the *Kirrel2* and *Rtp1* promoters. By contrast, we were unable to detect ATF5 binding on comparable regions of the *Olfr170* and *Olfr513* promoters.

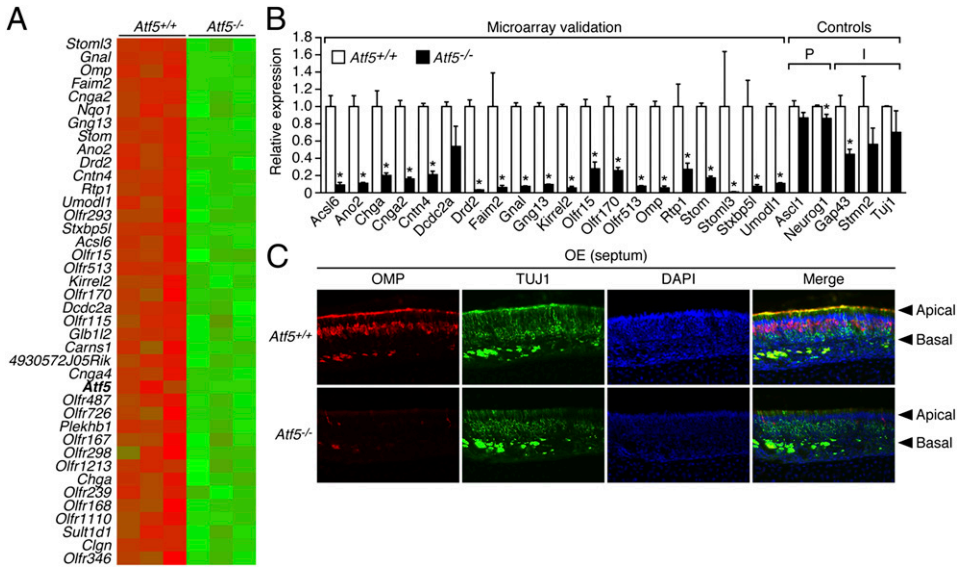

Fig. 4. ATF5 is required for terminal differentiation of OSNs. (*A*) Heat map displaying the 40 genes whose expression levels were most decreased in *Atf5*$^{-/-}$ OE (green) relative to that in *Atf5*$^{+/+}$ OE (red). (*B*) qRT-PCR monitoring gene expression in OE of P0 *Atf5*$^{+/+}$ and *Atf5*$^{-/-}$ mice. The results were normalized to the expression level in *Atf5*$^{+/+}$ mice, which was set to 1. P, progenitor markers; I, immature OSN markers. *$P < 0.05$. (*C*) Immunofluorescence monitoring OMP (red) and TUJ1 (green) staining in OE (from the septum) of P0 *Atf5*$^{+/+}$ and *Atf5*$^{-/-}$ mice. Sections were counterstained with DAPI (blue). Merged images are shown on the *Right*. Arrowheads indicate the apical and basal layers of the OE. Magnification 200×.

These collective results support the possibility that ATF5 directs transcription of some OSN-specific genes by direct binding to the target gene promoter.

Retinoic acid promotes olfactory identity and is required for olfactory function (18). Fig. 6*E* shows that, following treatment with retinoic acid, *Atf5*$^{+/-}$ murine neural stem cells stained positively for β-gal, indicative of *Atf5* expression. Consistent with this result, the qRT-PCR experiment of Fig. 6*F* shows that treatment of murine neural stem cells with retinoic acid resulted in the upregulation of *Atf5* as well as the OSN-specific genes *Kirrel2* and *Rtp1*. Notably, *Kirrel2* and *Rtp1* expression was unaffected by retinoic acid treatment of *Atf5*$^{-/-}$ neural stem cells. Thus, *Atf5* expression is activated by retinoic acid, an upstream inducer of OSN differentiation, and is required for retinoic acid-induced transcriptional activation of OSN-specific genes.

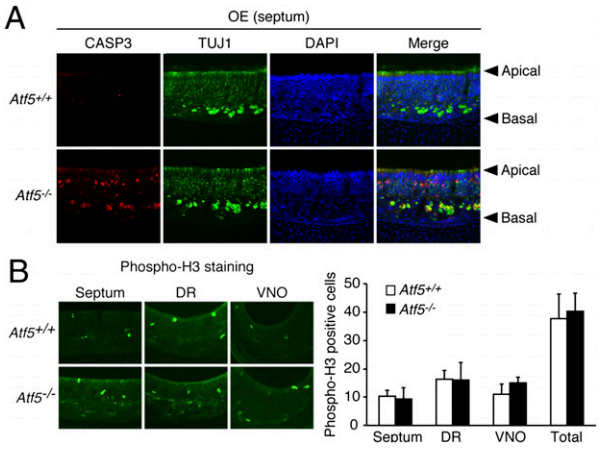

Fig. 5. ATF5 is critical for survival of mature OSNs. (*A*) Immunofluorescence monitoring cleaved caspase 3 (CASP3) (red) and TUJ1 (green) staining in OE (from the septum) of P0 *Atf5*$^{+/+}$ and *Atf5*$^{-/-}$ mice. Sections were counterstained with DAPI (blue). Merged images are shown on the *Right*. Arrowheads indicate the apical and basal layers of the OE. Magnification 200×. (*B*) (*Upper*) Immunofluorescence monitoring phosphorylated histone H3 (Phospho-H3) staining in the septum, dorsal region (DR), and VNO of newborn *Atf5*$^{+/+}$ and *Atf5*$^{-/-}$ mice. (*Right*) The average number of phospho-H3–positive cells in three different microscopic fields is indicated for each region.

Discussion

In this report, we study the physiological role of ATF5 and find that *Atf5*$^{-/-}$ mice die neonatally, which can be explained by an olfactory defect and a resultant competitive suckling deficit. The neonatal death phenotype that we observe is consistent with that described in previous studies in which genes required for olfactory function have been ablated in mice (12, 13, 19). On the basis of the *Atf5* expression pattern and effects of *Atf5* loss discussed below, we conclude that ATF5 is required for terminal differentiation and survival of the majority of OSNs in the OE. Whether ATF5 is also required for terminal differentation and survival of all OSN subtypes (reviewed in ref. 11) remains to be determined.

On the basis of β-gal activity in *Atf5*$^{+/-}$ mice and in situ hybridization we find that *Atf5* is highly and selectively expressed in the olfactory system. This conclusion is strongly supported by our observation that the only detectable phenotypic abnormality of *Atf5*$^{-/-}$ mice is a large reduction of mature OSNs in the OE. *Atf5* expression starts at E11.5, when the nose pit emerges, which is about 1 d after the olfactory pit forms and OSNs are first detected (8). Thus, the start of *Atf5* expression conincides with the emergence of OSNs from early progenitors. We have also shown that in murine neural stem cells *Atf5* expression is induced by retinoic acid, which promotes and is required for OSN differentiation (18). *Atf5* continues to be expressed in mature OSNs throughout adulthood, suggesting a continual role for ATF5 in olfactory function. We also detected ATF5 expression in VSNs; however, the role of ATF5 in the VNO will require further investigation.

Our microarray results revealed that the expression levels of many OSN-specific genes were substantially decreased in *Atf5*$^{-/-}$ OE. These genes include 172 *Olfr* genes and other genes, such as *Gnal* (12), *Rtp1* (20), and *Kirrel2* (21), that are critical for olfactory function. By contrast, genes expressed in OSN progenitors (*Ascl1* and *Neurog1*) were unaffected, and immature OSN-specific genes (*Gap43*, *Stmn2*, and *Tuj1*) were only modestly affected by loss of *Atf5*. Immunostaining enabled us to attribute the loss of OSN-specific gene expression in *Atf5*$^{-/-}$ OE to a massive reduction of mature OSNs. By contrast, the number of immature OSNs in OE

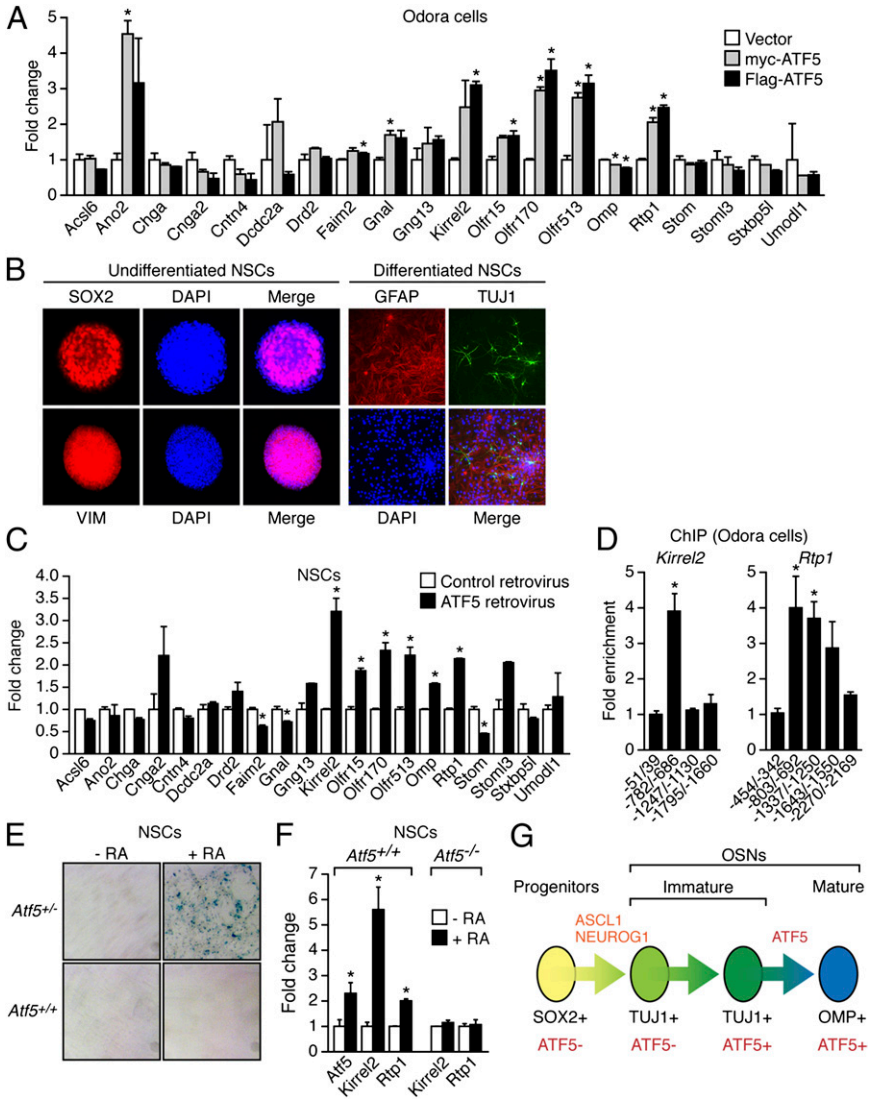

Fig. 6. ATF5 can direct OSN-specific gene expression. (*A*) qRT-PCR expression analysis of 20 genes in rat Odora cells transfected with myc-ATF5, Flag-ATF5, or empty vector. Fold change is relative to the vector control, which was set at a value of 1. (*B*) Immunofluorescence monitoring SOX2 and VIM staining in undifferentiated neural stem cells (NSCs) (*Left*) and GFAP and TUJ1 staining in differentiated NSCs (*Right*). Cells were counterstained with DAPI (blue). Merged images are shown. Magnification 200×. (*C*) qRT-PCR analysis monitoring expression of 20 genes in murine NSCs transduced with a retrovirus that expresses ATF5 or empty retrovirus. Fold change is relative to the empty retrovirus control, which was set at a value of 1. (*D*) ChIP analysis monitoring ATF5 binding to the promoters of *Kirrel2* and *Rtp1* in Odora cells. Fold enrichment is specified relative to nonspecific recruitment to a control gene desert locus, which was set to 1. Primer coordinates are given relative to the AUG start codon. (*E*) β-Gal staining of $Atf5^{+/+}$ or $Atf5^{+/-}$ NSCs induced to differentiate in the presence of 25 μM retinoic acid (RA). Magnification 20×. (*F*) qRT-PCR analysis monitoring expression of *Atf5* and *Kirrel2* in $Atf5^{+/+}$ and $Atf5^{-/-}$ NSCs in the presence and absence of RA. Fold change in expression is relative to the expression level in the absence of RA, which was set at 1. (*G*) Model for ATF5-directed differentiation of OSNs in the OE. $^*P < 0.05$.

was relatively unaffected by loss of *Atf5*. Thus, the reduced number of mature OSNs in $Atf5^{-/-}$ OE can be explained, at least in part, by a failure of immature OSNs to fully differentiate into mature OSNs. In support of this idea, we show that ATF5 can direct neural progenitor cells to express some mature OSN-specific genes. Perhaps not surprisingly, ectopic expression of ATF5 did not result in the transcriptional induction of all mature OSN-specific genes (Fig. 6*C*), indicating that factors in addition to ATF5 are required to convert neural progenitors into mature OSNs.

Our immunostaining results also revealed that *Atf5* is expressed in all mature OSNs and in some, but not all, immature OSNs. Collectively, our results suggest that *Atf5* is first expressed in immature OSNs and that the resultant ATF5 functions to promote differentation into mature OSNs (Fig. 6*G*). Previous studies have identified factors, such as ASCL1 and NEUROG1, that are required for the commitment of neural precursors to OSNs. To our knowledge, ATF5 is the only factor known to specifically act by promoting the conversion of immature to mature OSNs.

In the absence of *Atf5*, some OSNs were found to undergo apoptosis, which likely also contributes to the loss of mature OSNs in $Atf5^{-/-}$ OE. The ability of ATF5 to promote survival of mature OSNs may result from ATF5-directed transcriptional stimulation of anti-apoptotic gene (see, for examples, refs. 5 and 22). In support of this possibility, we found that the expression level of *Faim2*, which encodes a neuron-specific inhibitor of apoptosis (23), was dramatically decreased in $Atf5^{-/-}$ OE (Fig. 4*B*). However, previous studies have found that disruption of normal OSN differentiation can result in apoptosis (24–26). Thus, apoptosis induction in the absence of *Atf5* may also be explained by the inability of immature OSNs to fully differentiate into mature OSNs.

Materials and Methods

Mice. An $Atf5^{+/LacZ}$ embryonic stem cell clone was obtained from the National Institutes of Health Knockout Mouse Project repository, and its genomic structure was verified by long-fragment PCR and Southern blotting. The clone was microinjected into C57BL6-albino blastocysts and implanted into a pseudopregnant C57BL6-albino recipient mother to generate chimeric F0 founders, which were backcrossed to C57BL6 to generate $Atf5^{+/LacZ}$ F1 heterozygotes, which were intercrossed to generate $Atf5^{LacZ/LacZ}$ homozygotes (referred to as $Atf5^{-/-}$ here). Animal protocols were approved by the Institutional Animal Care and Use Committee at the University of Massachusetts Medical School.

Whole-Mount β-Gal Activity Assay. Tissues were dissected in 100 mM phosphate buffer (pH 7.4) and 2 mM $MgCl_2$ and fixed and stained (27). For Fig. 3*A*, horizontal tissue sections (16 μm) from a P0 mouse were cryopreserved without fixation, and a β-gal activity assay was performed followed by counterstaining with eosin.

Immunofluorescence. Dissected mouse heads were cryosectioned followed by immunofluorescence (28). Cells grown on glass coverslips (coated with poly-D-lysine/laminin for neural stem cells) were infected with virus or

transfected with plasmids and grown for an additional 60 h. Cells were washed with PBS, fixed in 4% (wt/vol) paraformaldehyde at 4 °C for 10 min, washed three times in PBS at room temperature, and incubated in blocking buffer for 1 h. Coverslips were incubated overnight as described above with the following primary antibodies: OMP (Wako Chemicals); TUJ1 (Covance); GAP43 (Millipore); β-galactosidase (MP Cappel); cleaved caspase-3 (Cell Signaling); phospho-histone H3 (Upstate); SOX2 (R&D System); GFAP (DAKO); and myc, Flag, and Vimentin-Cy3 (Sigma). Secondary antibodies were conjugated with Alexa Fluor 488, Alexa Fluor 594 (Invitrogen), and Cy3 or FITC (Jackson Laboratories) fluorophores. Nuclei were counterstained with DAPI (Molecular Probes). Images were acquired using a Zeiss AxioCam camera mounted to a Zeiss Axioplan immunofluorescence microscope.

Gene Expression Profiling. Olfactory septa and turbinates were dissected from *Atf5*$^{+/+}$ and *Atf5*$^{-/-}$ P0 pups ($n = 3$) from different litters and pooled into a single sample. Three independent samples were prepared for each genotype. Total RNA was isolated, and samples were hybridized to GeneChip Mouse Gene 1.0 ST Arrays (Affymetrix) and analyzed using Affymetrix software. RMA method (29, 30) in the Affy package from Bioconductor was used in R to summarize the probe-level data and normalize the dataset to remove across-array variation. A moderated *t* test in Limma package (31) was used to determine whether a gene's expression level differed between *Atf5*$^{+/+}$ and *Atf5*$^{-/-}$. Genes with a fold change ≥1.5 and a *P* value <0.001 were considered significant. The data discussed in this publication have been deposited in National Center for Biotechnology Information's Gene Expression Omnibus (GEO) (32) and are accessible through GEO accession no. GSE37609 (http://www.ncbi.nlm.nih.gov/geo/query/acc.cgi?acc=GSE37609).

qRT-PCR. Total RNA was extracted using TRIzol (Invitrogen). First-strand cDNA was synthesized using the ImProm-II Reverse Transcription System (Promega). qRT-PCR was performed with gene-specific primers using the ABI Prism 7700 Sequence Detector System (Applied Biosystems) (28) using *Gapdh* or *Rpl41* as an internal control.

Embryonic Neural Stem Cell Culture. Lateral and medial ganglionic eminences were dissected from the forebrains of E14 mouse embryos and collected in PBS with 2% (wt/vol) glucose on ice. Tissues were dissociated by triturating with a micropipette. Undifferentiated neural stem cells (NSCs) were maintained as neurospheres in NSC growth medium (DMEM/F-12, 100 μg/mL transferrin, 5 μg/mL insulin, 20 nM progesterone, 10 μM putrescine, 30 nM selentine) in the presence of 20 ng/mL EGF (StemCell Technologies). NSCs were differentiated in NSC Basal Medium plus Differentiation Supplement (StemCell Technologies). For retinoic acid treatment, NSCs were grown on plates coated with poly(D) lysine and aminin (Sigma) and incubated with 20 μM retinoic acid in differentiation medium for 48 h. Cells were fixed and stained for β-gal activity or harvested for total RNA extraction and qRT-PCR.

Ectopic *Atf5* Expression. Odora cells were cultured in DMEM with 10% (vol/vol) FBS and 7% (vol/vol) CO_2 at 33 °C. Cells were transfected with pFLAG-CMV-ATF5 or pCS2-Myc-ATF5, constructed by amplifying *Atf5* by RT-PCR and cloning it into p3XFlag-myc-CMV-26 (Sigma) or pCS2-MT (33), respectively, or empty vector using Nucleofector Kit V and program T-028 (Lonza). After 72 h, cells were processed for gene expression, ChIP, or immunofluorescence.

ChIP Assays. pCS2-Myc-ATF5–transfected Odora cells were fixed with 1% (wt/vol) formaldehyde for 10 min at 25 °C and then stopped with 0.125 M glycine, followed by a standard ChIP assay (34) using nonimmune mouse IgG (Santa Cruz) or anti-myc mouse monoclonal antibody (Sigma). ChIP DNA and input DNA were used as templates for qPCR.

Statistical Analysis. All experiments were performed at least three times. Mean values for individual experiments are expressed as mean ± SD. *P* values were calculated using the log-rank test in the survival package in R (35) (Fig. 1*B*) or the Welch two-sample *t* test (Figs. 1*D*, 4*B*, 5*B*; and 6 *A*, *C*, *D*, and *F*; and Figs. S1*D*, S6*A*, and S7*B*). A *P* value <0.05 was considered significant.

ACKNOWLEDGMENTS. We thank James Schwob for providing Odora cells. This work is supported by National Institutes of Health Grant R01CA115817 (to M.R.G.). M.R.G. is an investigator of the Howard Hughes Medical Institute.

1. Persengiev SP, Green MR (2003) The role of ATF/CREB family members in cell growth, survival and apoptosis. *Apoptosis* 8(3):225–228.
2. Devireddy LR, Teodoro JG, Richard FA, Green MR (2001) Induction of apoptosis by a secreted lipocalin that is transcriptionally regulated by IL-3 deprivation. *Science* 293 (5531):829–834.
3. Persengiev SP, Devireddy LR, Green MR (2002) Inhibition of apoptosis by ATFx: A novel role for a member of the ATF/CREB family of mammalian bZIP transcription factors. *Genes Dev* 16(14):1806–1814.
4. Monaco SE, Angelastro JM, Szabolcs M, Greene LA (2007) The transcription factor ATF5 is widely expressed in carcinomas, and interference with its function selectively kills neoplastic, but not nontransformed, breast cell lines. *Int J Cancer* 120(9):1883–1890.
5. Sheng Z, et al. (2010) A genome-wide RNA interference screen reveals an essential CREB3L2-ATF5-MCL1 survival pathway in malignant glioma with therapeutic implications. *Nat Med* 16(6):671–677.
6. Angelastro JM, et al. (2005) Downregulation of activating transcription factor 5 is required for differentiation of neural progenitor cells into astrocytes. *J Neurosci* 25 (15):3889–3899.
7. Mason JL, et al. (2005) ATF5 regulates the proliferation and differentiation of oligodendrocytes. *Mol Cell Neurosci* 29(3):372–380.
8. Treloar HB, Miller AM, Ray A, Greer CA (2010) *Development of the Olfactory System: The Neurobiology of Olfaction*, ed Menini A (CRC Press, Boca Raton, FL).
9. Carter LA, MacDonald JL, Roskams AJ (2004) Olfactory horizontal basal cells demonstrate a conserved multipotent progenitor phenotype. *J Neurosci* 24(25):5670–5683.
10. Cheng LE, Reed RR (2007) Zfp423/OAZ participates in a developmental switch during olfactory neurogenesis. *Neuron* 54(4):547–557.
11. Munger SD, Leinders-Zufall T, Zufall F (2009) Subsystem organization of the mammalian sense of smell. *Annu Rev Physiol* 71:115–140.
12. Belluscio L, Gold GH, Nemes A, Axel R (1998) Mice deficient in G(olf) are anosmic. *Neuron* 20(1):69–81.
13. Brunet LJ, Gold GH, Ngai J (1996) General anosmia caused by a targeted disruption of the mouse olfactory cyclic nucleotide-gated cation channel. *Neuron* 17(4):681–693.
14. Wong ST, et al. (2000) Disruption of the type III adenylyl cyclase gene leads to peripheral and behavioral anosmia in transgenic mice. *Neuron* 27(3):487–497.
15. Voyron S, et al. (1999) Apoptosis in the development of the mouse olfactory epithelium. *Brain Res Dev Brain Res* 115(1):49–55.
16. Cowan CM, Roskams AJ (2002) Apoptosis in the mature and developing olfactory neuroepithelium. *Microsc Res Tech* 58(3):204–215.
17. Murrell JR, Hunter DD (1999) An olfactory sensory neuron line, odora, properly targets olfactory proteins and responds to odorants. *J Neurosci* 19(19):8260–8270.
18. Rawson NE, LaMantia AS (2006) Once and again: retinoic acid signaling in the developing and regenerating olfactory pathway. *J Neurobiol* 66(7):653–676.
19. Guillemot F, et al. (1993) Mammalian achaete-scute homolog 1 is required for the early development of olfactory and autonomic neurons. *Cell* 75(3):463–476.
20. Saito H, Kubota M, Roberts RW, Chi Q, Matsunami H (2004) RTP family members induce functional expression of mammalian odorant receptors. *Cell* 119(5):679–691.
21. Serizawa S, et al. (2006) A neuronal identity code for the odorant receptor-specific and activity-dependent axon sorting. *Cell* 127(5):1057–1069.
22. Dluzen D, Li G, Tacelosky D, Moreau M, Liu DX (2011) BCL-2 is a downstream target of ATF5 that mediates the prosurvival function of ATF5 in a cell type-dependent manner. *J Biol Chem* 286(9):7705–7713.
23. Reich A, et al. (2011) Fas/CD95 regulatory protein Faim2 is neuroprotective after transient brain ischemia. *J Neurosci* 31(1):225–233.
24. Duggan CD, DeMaria S, Baudhuin A, Stafford D, Ngai J (2008) Foxg1 is required for development of the vertebrate olfactory system. *J Neurosci* 28(20):5229–5239.
25. Murray RC, Navi D, Fesenko J, Lander AD, Calof AL (2003) Widespread defects in the primary olfactory pathway caused by loss of Mash1 function. *J Neurosci* 23(5):1769–1780.
26. Hirota J, Mombaerts P (2004) The LIM-homeodomain protein Lhx2 is required for complete development of mouse olfactory sensory neurons. *Proc Natl Acad Sci USA* 101(23):8751–8755.
27. Gogos JA, Osborne J, Nemes A, Mendelsohn M, Axel R (2000) Genetic ablation and restoration of the olfactory topographic map. *Cell* 103(4):609–620.
28. Wang SZ, et al. (2006) An oligodendrocyte-specific zinc-finger transcription regulator cooperates with Olig2 to promote oligodendrocyte differentiation. *Development* 133 (17):3389–3398.
29. Irizarry RA, et al. (2003) Exploration, normalization, and summaries of high density oligonucleotide array probe level data. *Biostatistics* 4(2):249–264.
30. Irizarry RA, et al. (2003) Summaries of Affymetrix GeneChip probe level data. *Nucleic Acids Res* 31(4):e15.
31. Smyth GK (2004) Linear models and empirical bayes methods for assessing differential expression in microarray experiments. *Stat Appl Genet Mol Biol* 3:Article3.
32. Edgar R, Domrachev M, Lash AE (2002) Gene Expression Omnibus: NCBI gene expression and hybridization array data repository. *Nucleic Acids Res* 30(1):207–210.
33. Roth MB, Zahler AM, Stolk JA (1991) A conserved family of nuclear phosphoproteins localized to sites of polymerase II transcription. *J Cell Biol* 115(3):587–596.
34. Sheng Z, Wang SZ, Green MR (2009) Transcription and signalling pathways involved in BCR-ABL-mediated misregulation of 24p3 and 24p3R. *EMBO J* 28(7):866–876.
35. Ihaka R, Gentleman R (1996) R: A language for data analysis and graphics. *J Comput Graph Statist* 5(3):299–314.